Desalination and Water Treatment
www.deswater.com

doi: 10.5004/dwt.2018.21833

102 (2018) 280–288
January

Biosorption of reactive red-120 dye onto fungal biomass of wild *Ganoderma* stipitatum

P.S.C. Souza[a,*], J. Santos[b], A.R. Souza[c], L. Spessato[a], O. Pezoti[a], H.J. Alves[b], N.B. Colauto[d], V.C. Almeida[a,*], D.C. Dragunski[e]

[a]*Laboratory of Environmental and Agrochemistry, Department of Chemistry, Estate University of Maringá, 5790 Colombo Ave., CEP 87020-900 – Maringá, Paraná, Brazil, Tel. +554430114500; Fax: +554430114449; emails: patricia.carraro@hotmail.com (P.S.C. Souza), vcalmeida@uem.br (V.C. Almeida), lucas.spessato@hotmail.com (L. Spessato), pezotinho@hotmail.com (O. Pezoti)*
[b]*Laboratory of Chemistry and Soil Fertility and Laboratory of Catalysis and Biofuel Production, Federal University of Paraná, 2153 Pioneiro St., CEP 85950-000 – Palotina, Paraná, Brazil, Tel. +554432111317; email: joe.dossantos@hotmail.com (J. Santos), Tel: +554432118500; Fax: +554432118511; email: helquimica@gmail.com (H.J. Alves)*
[c]*Laboratory of Kinetics and Applied Thermodynamics, Federal University of Paraná, 100 Franscisco Heraclito dos Santos St., CEP 81531-990 – Curitiba, Paraná, Brazil, Tel. +554133613151; Fax: +554133613674; email: ariadinesouza@msn.com*
[d]*Laboratory of Molecular Biology, Paranaense University, 4282 Mascarenhas de Moraes Square., CEP 87502-210, Umuarama, Paraná, Brazil, Tel. +554436212828; email: nbc@prof.unipar.br*
[e]*State University of Western Paraná, 645 Rua da Faculdade St., CEP 85903-000, Toledo, Paraná, Brazil, Tel. +554533797142; Fax: +554533790002; email: dcdragunski@gmail.com*

Received 12 August 2017; Accepted 19 December 2017

ABSTRACT

In the present work, the reactive red 120 dye (red-120) biosorption onto fungal biomass (FB) of wild *Ganoderma* stipitatum basidiocarps was studied. The chemical and morphological characterization of FB was performed from Fourier transform infrared spectroscopy, scanning electron microscopy, pH at point of zero charge (PH_{PZC}) and BET surface area. According to biosorption studies, the highest value of biosorption capacity was found at pH 3.0. The kinetic experimental data were best described by Elovich model suggesting the existence of a chemisorption process. The biosorption equilibrium data were best fitted by Langmuir isotherm model presenting maximum monolayer biosorption capacity of 44.44 mg g^{-1}. Additionally, the thermodynamic studies indicated the biosorption of red-120 onto FB is spontaneous and exothermic. Therefore, FB may be considered a promising biosorbent for red-120 dye removal from the wastewaters.

Keywords: Biosorbent; Textile dye; Adsorption; Fungi

1. Introduction

Numerous synthetic dyes have been used in industrial sectors such as textiles, cosmetics, plastics, food, paper, among others, in order to impart color to manufactured products. The unrestrained use of these dyes can lead to serious environmental problems since 1%–10% are eliminated from industrial processes, and when not properly treated, it can reach natural water sources and consequently affect the environment [1]. Reactive synthetic dyes have chemical properties which lead them to be considered toxic and carcinogenic, besides being recalcitrant [2].

The reactive red-120 (red-120) is one of the most used reactive dyes in textile industry. It belongs to the class of azo dyes, presenting on its molecular structure several chemical groups such as azo (–N=N–), chlorotriazine (C_3N_3Cl), naphthalene ($C_{10}H_8$), aniline (C_6H_7N) and sulfonic (SO_3^-), and it

* Corresponding author.

has high solubility in water with low biodegradability [3]. Many technologies have been employed for the remediation of synthetic dyes in wastewater [1]. Usually, these processes consist of conventional aerobic or anaerobic methods [4], ultrafiltration, nanofiltration [5], non-conventional methods such as photoelectrocatalysis [6] and photo-Fenton [7]. Most of these methods have advantages, such as low cost and easy application. On the other hand, their disadvantages are associated to partial removal of dyes or formation of by-products, which may lead to toxicity, causing new problems related to their final disposal [8].

The adsorption process is considered an alternative for removal of emerging pollutants in wastewater due to its efficiency, ease of operation, and absence of toxicity by adsorbents/biosorbents. Thus, several studies have been carried out which the purpose of is to find new adsorbent materials with good performance for adsorption processes. In this perspective, the biomasses of several fungi including *Aspergillus niger*, *Rhizopus arrhizus*, *Rhizopus oryzae*, among others were applied for removal of dyes from aqueous solutions [9–12]. However, for the best of our knowledge, the use of fungal biomass (FB) of wild *Ganoderma* genus for removing reactive azo dyes has not been reported in the literature. The *Ganoderma* stipitatum grows naturally in tree stumps and produce large basidiocarps. Therefore, the aim of this study was to investigate the removal of red-120 dye using FB of *Ganoderma* stipitatum basidiocarps as biosorbent.

2. Materials and methods

2.1. Chemicals

All chemicals used in this study were of analytical grade. Red-120 dye (Fig. 1, $C_{44}H_{30}Cl_2N_{14}O_{20}S_6Na_6$, MW: 1 475 g mol^{-1}) was kindly provided by Sintex Tinturaria Industrial Ltda (Goioerê-PR, Brazil). A stock solution of 1,000 mg L^{-1} was prepared by dissolving 1.0 g of dry red-120 in 1.0 L of distilled water. The working solutions were prepared from dilution of stock solution. The pH values of solutions were adjusted using HCl and NaOH solutions (0.10 mol L^{-1}).

2.2. Preparation of biosorbent

Basidiocarps of a wild *Ganoderma* stipitatum were collected from a Sibipiruna tree stump (*Caesalpinia pluviosa*), then, they were dried in an oven with air circulation at 60°C for 12 h and ground in a Wiley knife mill (Marconi®). The obtained material was granulometrically separated, using a Tyler sieve of 10 mesh, and fungi biomass (FB) particles of 1.70 mm sizes were used as biosorbent. The FB was properly stored and cryopreserved according to Colauto et al. [13].

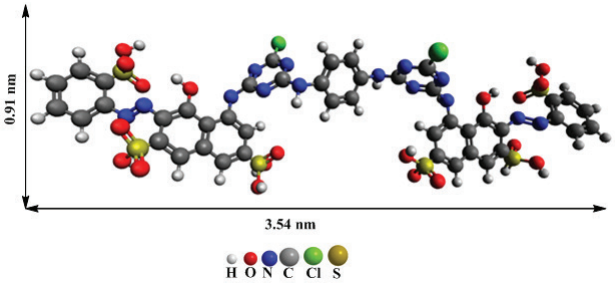

Fig. 1. Molecular structure of red-120 dye.

2.3. Characterization of biosorbent

The identification of functional groups present in FB was performed by Fourier transform infrared spectroscopy (FTIR) using a Shimadzu 8300 spectrometer. FTIR spectra were recorded with resolution of 4 cm^{-1} and acquisition rate of 32 scan min^{-1} for wavenumbers ranging from 4,000 to 400 cm^{-1}. The KBr pellets were prepared in the ratio of 1:100 by mixing 1.0 mg of FB with 100 mg of KBr, and then pressed at 5 ton cm^2 for 2.5 min.

The textural properties were characterized from the N_2 adsorption/desorption isotherms at 77 K using a surface area analyzer (Quantachrome® Nova1200). The specific surface area (S_{BET}) of biosorbent was determined by Brunauer–Emmett–Teller equation (BET) [14] at relative pressure (P/P^0) between 0.05 and 0.20. The total pore volume (V_T) was calculated as the maximum amount of nitrogen adsorbed at relative pressure of $P/P^0 = 0.99$. The micropore volume (V_μ) was determined using De Boer method [15] and the mesopore volume (V_m) obtained from the difference between total pore volume and micropore volume ($V_T - V_\mu$). The average pore diameter (D_p) was determined by the ratio $4V_T/S_{BET}$, and pore size distribution from Barret–Joyner–Halenda method (BJH) which refers to mesoporous materials [16].

The morphological characterization of FB was performed by scanning electron microscopy (SEM). SEM images were obtained by a Tescan® model Vega3 instrument operating at 30 kV. For sample preparation, FB particles were fixed in an aluminum support by a carbon tape and covered with a thin layer of gold.

The pH at point of zero charge (PH_{PZC}) of the FB was determined from the pH_{drift} method reported by Prahas et al. [17]. The pH_{PZC} was evaluated by preparing NaCl solutions (0.01 mol L^{-1}) at pH range of 2.0 to 8.0, which were adjusted with NaOH and HCl (0.10 mol L^{-1}). Then, 0.50 g of biosorbent was added into Erlenmeyer flasks containing 50.0 mL of NaCl solutions with respective pH values. These suspensions were constantly stirred at 25°C for 24 h. The final pH of each solution was measured using a pH meter (Tecnal® TEC-2). Finally, the pH_{PZC} of FB was determined from the plot of ΔpH ($pH_{final} - pH_{initial}$) vs. $pH_{initial}$.

2.4. Biosorption experiments

The biosorption studies were performed by batch systems. Thus, 0.50 g of FB was added into Erlenmeyer flasks containing 50.0 mL of red-120 solutions. Then, the suspensions were placed on a rotary shaker (Solab® SL-221) and stirred under 90 rpm for predetermined time at 25°C. After stirring, the samples were centrifuged (3,000 rpm) for 10 min and filtered. The remaining concentrations of red-120 were determined by UV–Vis spectrophotometer (Shimadzu® 1800) at wavelength of maximum absorbance (λ_{max} = 543 nm) using a calibration curve (1–100 mg L^{-1}).

The pH effect on the biosorption of red-120 onto FB was investigated using red-120 solutions (50 mg L^{-1}) at pH range of 3.0–10.0 and stirring time of 24 h. The biosorption capacity values, q_m (mg g^{-1}), the amount adsorbed at the equilibrium,

q_e (mg g^{-1}), and the adsorbed amount of red-120 at time t onto FB, q_t (mg g^{-1}), were calculated according to Eq. (1):

$$q_m = q_e = q_t = \frac{(C_0 - C_{e,t})V}{W} \quad (1)$$

where V is the solution volume (L), C_0 is the initial concentration of red-120 dye (mg L^{-1}), C_t is the red-120 dye liquid phase concentration at time t and C_e is concentration at equilibrium, and W is the dry mass of biosorbent (g).

The effect of contact time on the biosorption of red-120 onto FB was evaluated from kinetic studies. Thus, red-120 solutions (50 mg L^{-1}) were placed in contact with FB and stirred at 25°C for a time interval ranging from 5 to 1,440 min. The biosorption capacities at time t (q_t) were determined from Eq. (1). The non-linear kinetic models of pseudo-first order, pseudo-second order and Elovich were adjusted to experimental biosorption data as well as the intraparticle diffusion model which are presented in Table 1.

The biosorption equilibrium was investigated from biosorption isotherm which was obtained from red-120 solutions at pH = 3.0 with initial concentrations ranging from 30 to 1,000 mg L^{-1} and stirring time of 540 min. The biosorption capacities at equilibrium (q_e) were calculated from Eq. (1). The non-linear isotherm models of Langmuir and Freundlich applied to experimental data are shown in Table 2.

Table 1
Biosorption kinetic models

Model	Equation	Reference
Pseudo-first order	$q_t = q_e[1 - e^{-k_1 t}]$	[18]
Pseudo-second order	$q_t = \frac{k_2 q_e^2 t}{1 + k_2 q_e t}$	[19]
Elovich	$q_t = \frac{1}{\beta}\ln(1 + \alpha\beta t)$	[20]
Intraparticle diffusion	$q_t = k_{di}\sqrt{t}$	[21]

k_1 and k_2 are the biosorption rate constants of pseudo-first order and pseudo-second order, respectively; α and β are the constants of Elovich; K_{di} is the intraparticle diffusion rate constant.

Table 2
Biosorption isotherm models

Model	Equation	Reference
Langmuir	$q_e = \frac{Q_m k_a C_e}{1 + k_a C_e}$	[22]
	$R_L = \frac{1}{1 + K_a C_0}$	
Freundlich	$q_e = k_F C_e^{1/n_F}$	[23]

Q_m is the maximum biosorption capacity; k_a is the Langmuir constant; k_F and n_F are the Freundlich constants.

2.4.1. Evaluation of models

The kinetic and isotherm modeling were performed using Origin® 8.5 software. The applicability of the models to describe the experimental biosorption data was evaluated from the determination coefficients (R^2) and normalized standard deviations (Δq_e), which were determined according to Eq. (2):

$$\Delta q_e(\%) = 100\sqrt{\frac{\sum[(q_{e,\exp} - q_{e,\text{cal}})/q_{e,\exp}]^2}{n-1}} \quad (2)$$

where $q_{e,\exp}$ is the experimental biosorption capacity (mg g^{-1}), $q_{e,\text{cal}}$ is the calculated biosorption capacity (mg g^{-1}) and n is the number of data points.

2.4.2. Thermodynamic studies

Thermodynamic studies were carried out ranging the temperature of biosorption system from 25°C to 65°C (C_0 = 50 mg L^{-1}, shaking time = 540 min). The energies involved in the process, such as entropy change ($\Delta S°$, J mol^{-1}K^{-1}), enthalpy change ($\Delta H°$, J mol^{-1}) and Gibbs free energy change ($\Delta G°$, J mol^{-1}), were estimated from the following equations [24]:

$$K_D = \frac{q_e}{C_e} \quad (3)$$

$$K_c = \frac{q_e}{C_e} \times 1000 \quad (4)$$

$$\Delta G° = -RT\ln(K_c) \quad (5)$$

$$\ln(K_c) = -\frac{\Delta H°}{RT} + \frac{\Delta S°}{R} \quad (6)$$

where R is the universal gas constant (8.314 J mol^{-1} K^{-1}), T is the absolute temperature (K), K_D is the variation of solute between the solid and liquid phases at equilibrium (L g^{-1}) and K_c is a dimensionless constant, used to standardize the thermodynamic equilibrium constant [25].

The $\Delta G°$ values were obtained from K_c values for each temperature, being this energy considered as the difference between the enthalpy change and the entropy change at a constant temperature [26]. The $\Delta H°$ and $\Delta S°$ values were calculated using the van't Hoff equation (Eq. (6)).

3. Results and discussion

3.1. Characterization of biosorbent

FTIR analyses were performed in order to investigate the presence of chemical groups on biosorbent. Fig. 2 shows the FTIR spectra of red-120 dye and FB of *Ganoderma* stipitatum.

Analyzing the FTIR spectrum of red-120 (Fig. 2(a)), the band centered at 3,450 cm^{-1} can be attributed to O–H and

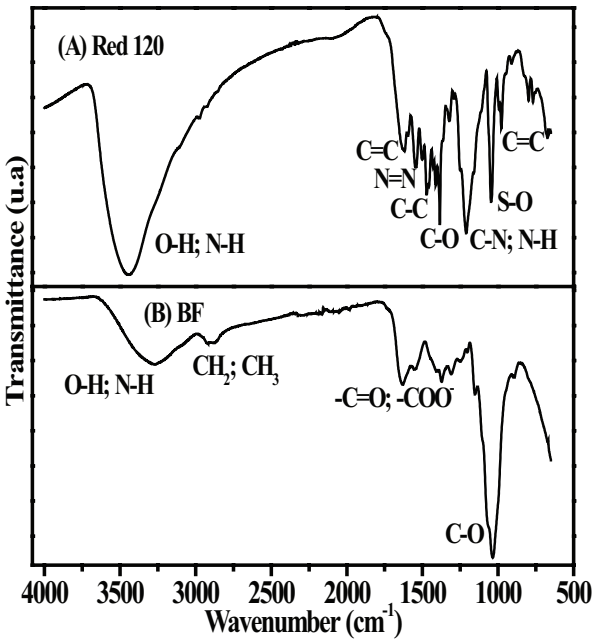

Fig. 2. FTIR spectra of red-120 dye (A) and FB from *Ganoderma* stipitatum (B).

N–H stretching of hydroxyl and aniline groups, respectively. The bands at 1,621 and 982 cm^{-1} may be associated with C=C of aromatic groups [27], while the band at 1,545 cm^{-1} identify the N=N stretching, which is characteristic of azo group [28]. The bands at 1,470; 1,380 and 1,208 cm^{-1} can be assigned to C–C, C–O, C–H and N–H bonds, respectively [29], and the band at 1,041 cm^{-1} to S–O stretching [30].

From FTIR spectrum of FB (Fig. 2(b)), it can be seen a broader band at 3,290 cm^{-1}, which can be attributed to characteristic vibrations of O–H symmetric stretching and N–H of triterpenes and polysaccharides [31]. The band at 2,887 cm^{-1} can be ascribed to symmetric and asymmetric stretching of CH_3 and CH_2 while the band at 1,622 cm^{-1} can be assigned to C=O stretching vibration and –COO– of carbonyl groups [32]. In addition, the band at 1,036 cm^{-1} can be associated with C–N–C belonging to the asymmetric vibration of an aromatic compound [33].

3.1.1. Textural properties of biosorbent

Fig. 3 shows the N_2 adsorption and desorption isotherms of FB at 77 K, which can provide information regarding the textural properties such as specific surface area, total pore volume, micropore volume and average pore diameter. According to the IUPAC, N_2 adsorption/desorption isotherms of FB can be classified as type III, which is characteristic of materials with low porosity [34]. The textural parameters of FB are presented in Table 3.

The results demonstrate that FB has a low total pore volume (V_T = 0.03 $cm^3\ g^{-1}$) due to the absence of a well-developed porous structure. FB showed S_{BET} of 21.2 $m^2\ g^{-1}$ being higher than other biosorbents reported in the literature, such as chitin/lignin [35] and *Oreochromis niloticus* fish scales [36] which presented surface areas of 2.26, 2.11 and 2.06 $m^2\ g^{-1}$, respectively.

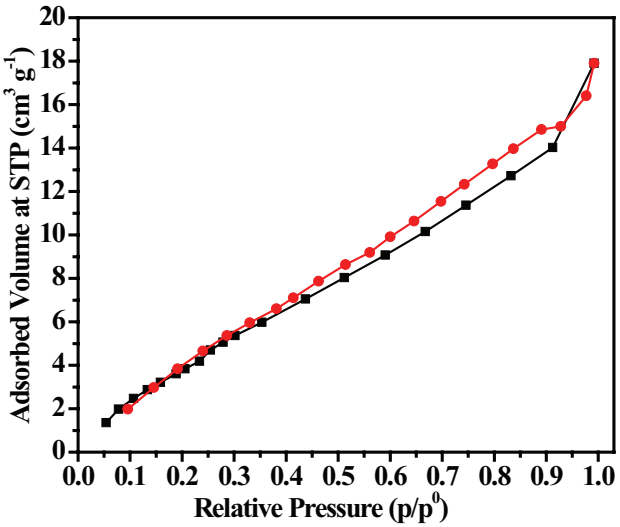

Fig. 3. N_2 adsorption (square symbols) and desorption (circular symbols) isotherms of FB at 77 K.

Table 3
Textural properties of FB

	S_{BET} ($m^2\ g^{-1}$)	V_T ($cm^3\ g^{-1}$)	V_μ ($cm^3\ g^{-1}$)	$V_{M/BJH}$ ($cm^3\ g^{-1}$)	D_p (nm)
FB	21.2	0.03	0.00	0.02	2.62

S_{BET} = BET surface area; V_T = total pore volume; V_μ = micropore volume; $V_{M/BJH}$ = mesopore volume calculated by BJH method; D_p = average pore diameter.

3.1.2. Scanning electron microscopy analysis

The SEM was carried in order to evaluate surface morphology of FB. From the SEM micrograph shown in Fig. 4, it can be verified that FB consists of a filaments structure, known as hyphae, which does not show uniformity each other with irregular surface that may be due to the production of lignolytic enzymes characteristics of *Ganoderma* stipitatum since the enzymatic activities of this fungus may vary according to different strains and culture conditions [37].

As observed in FTIR spectrum, the FB presents functional groups on its surface which can gain or lose protons causing a variation in the net charge of surface according to pH of solutions [38]. The pH_{PZC} can be defined as the pH value at which the surface net charge of a material is equal to zero [39]. Thus, in case of solutions with pH values lower than pH_{PZC}, the material surface will have the predominance of positive charges; on the other hand, for solutions with pH values higher than pH_{PZC}, the net charge of surface will be predominantly negative [40]. From Fig. 5, it can be seen that FB exhibited pH_{PZC} of 6.5, indicating the slightly acid characteristic of material.

3.2. Biosorption studies

3.2.1. Effect of pH

The pH of solution is considered as an important factor in biosorption process which affects biosorbent surface charge

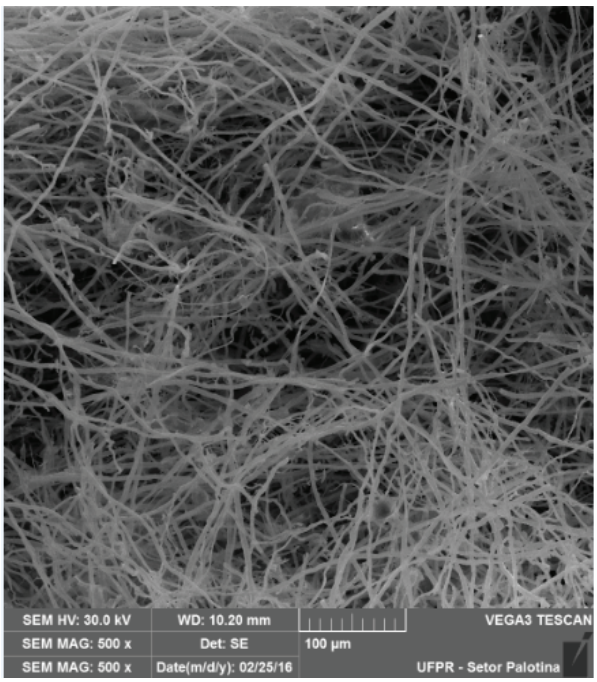

Fig. 4. SEM micrograph of FB.

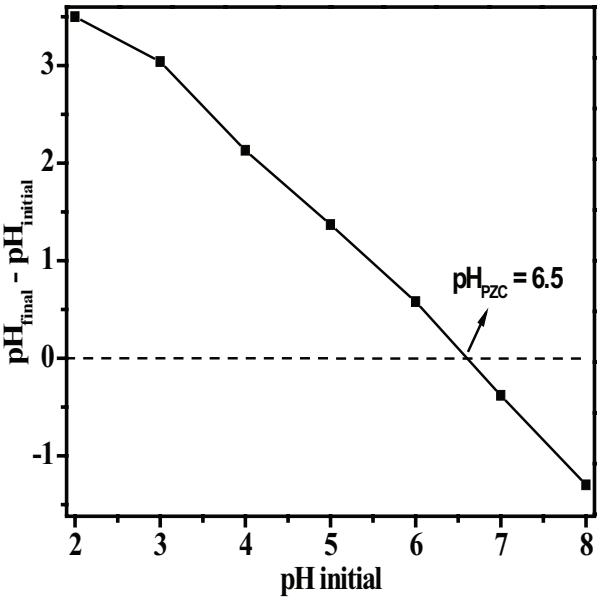

Fig. 5. pH at point of zero charge (pH_{PZC}) of FB.

and dye solubility [41]. Fig. 6 shows the effect of pH on the biosorption of red-120 onto FB.

As can be observed in Fig. 6, the higher values of Q_m were obtained at low pH values, once in acidic medium the FB has positive charge and red-120 negative charges, enhancing the electrostatic interaction between biosorbent and adsorbate. The improvement in the biosorption capacity may be related to the carbonyl (C=O) and hydroxyl (OH) groups present in the FB since the oxygen in these groups can act as a strong Lewis base being capable of interacting with the dye ions [38]. Thus, the pH = 3.0 was chosen for subsequent studies.

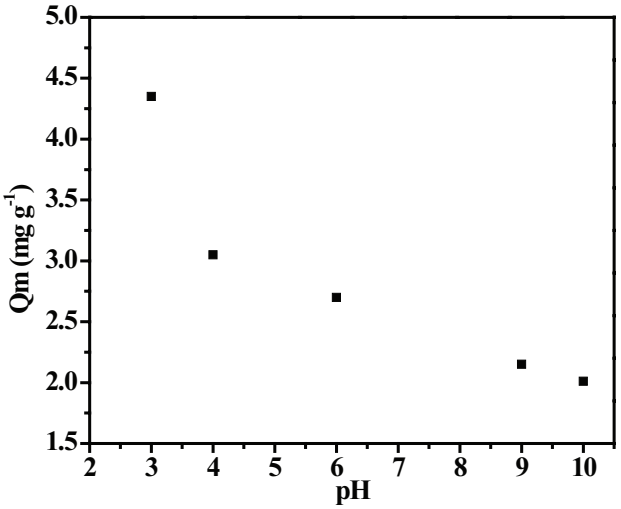

Fig. 6. Effect of pH on the biosorption of red-120 onto FB.

3.2.2. Biosorption kinetics

The biosorption kinetics of red-120 onto FB, as well as the non-linear adjustments of pseudo-first order, pseudo-second order and Elovich models is shown in Fig. 7. The results demonstrated that the system presented higher rate of biosorption in the first 120 min. In addition, the time required to reach the biosorption equilibrium (400 min) was relatively low, when compared with other types of fungi applied for removal of textile dyes [42,43].

The kinetic parameters regarding the biosorption of red-120 onto FB are displayed in Table 4. The results demonstrated that the Elovich model was best fitted to experimental kinetic data, presenting the highest value of R^2 (0.9890) besides the lowest value of Δq_e (3.01). The Elovich model suggests the existence of chemisorption process on an energetically heterogeneous surface without any effect of the interactions between adsorbed species and/or the desorption process [44]. The parameters α and β of Elovich model correspond to the initial biosorption rate (mg g^{-1} min^{-1}) and the desorption rate (g mg^{-1}), respectively. The values of α and β were of 2,740.4 and 3.36, respectively, indicating an effective interaction between red-120 and FB [45], and the viability of the process [46] besides the practically irreversible character of the system [47].

The adsorption mechanism can occur from three sequential steps: (i) external diffusion of the adsorbate through the boundary layer of biosorbent surface, (ii) intraparticle diffusion and (iii) adsorption of adsorbate onto active sites of biosorbent [48]. The importance of these steps in the biosorption of red-120 onto FB was investigated by applying the intraparticle diffusion model. Fig. 8 shows the graphic of q_t vs. $t^{1/2}$ and the linear adjustments for red-120 biosorption data while the kinetic parameters are listed in Table 5.

According to Fig. 8, it is possible to observe three define stages. The first one presenting the highest slope (k_{d1} = 1.47), followed by the second one (k_{d2} = 0.110) and the third one (k_{d3} = 0.010). The linear relationship of intraparticle diffusion model was not obeyed, demonstrating that more than one stage is involved in the biosorption mechanism [49,50]. The line segment corresponding to the second stage does not pass

through the origin, suggesting intraparticle diffusion may be involved, although it is not the rate-limiting step of biosorption process [51].

In order to evaluate the resistance to intraparticle diffusion, the intercept *C* (Table 5) of each stage was investigated and followed the relation $C_1 < C_2 < C_3$, indicating that in first instants the resistance to external diffusion is lower, and as contact time increase the amount of free dye molecules in solution decreases, since most of the molecules were retained onto FB due to biosorption. Thus, as the biosorption sites of FB are filled, the mobility of red-120 molecules becomes more difficult resulting in an increase in diffusion resistance at the next stage [52].

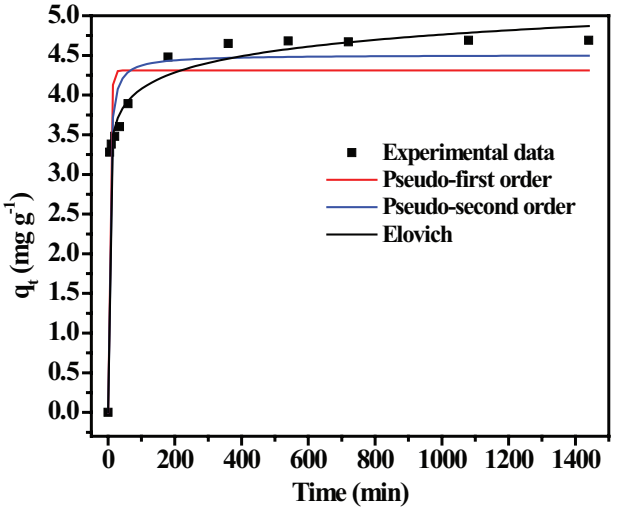

Fig. 7. Biosorption kinetics of red-120 onto FB and non-linear adjustments of pseudo-first order, pseudo-second order and Elovich models.

Table 4
Kinetic parameters for the biosorption of red-120 onto FB

C_0 (mg L^{-1})	$q_{e,exp}$ (mg g^{-1})	Pseudo-first order	Pseudo-second order	Elovich
50	4.68	q_e = 4.31	q_e = 4.51	α = 2,740.4
		k_1 = 0.22	k_2 = 0.07	β = 3.37
		h_0 = 0.94	h_0 = 1.47	
		R^2 = 0.8663	R^2 = 0.9396	R^2 = 0.9890
		Δq_e = 8.90	Δq_e = 6.16	Δq_e = 3.01

q_e = mg g^{-1}; k_1 = min^{-1}; k_2 = g mg^{-1} min^{-1}; h_0 = mg g^{-1} min^{-1}; Δq_e = %; α = mg g^{-1} min^{-1}; β = g mg^{-1}.

3.2.3. Biosorption isotherm

The isotherms are useful to evaluate the adsorption process as a unit operation providing information regarding the maximum adsorption capacities of various adsorbents/biosorbents [53]. In order to explore the biosorption equilibrium of red-120 onto FB, the isotherm models of Langmuir and Freundlich were fitted to experimental data and their non-linear adjustments are shown in Fig. 9(a).

The Langmuir model [22] describes an adsorption process that occurs on surfaces with homogeneous adsorption sites where each adsorbate molecule occupies one site and the maximum adsorption capacity occurs with formation of the monolayer [54]. The Freundlich model [23] is an empiric equation that describes the adsorption process with high degrees of heterogeneity suggesting it can occur in multilayers at sites with different adsorption energies which can decrease exponentially as the adsorbate is retained on the adsorbent surface. The Freundlich constant (n_F) is important to assess the favorability of adsorption process indicating the occurrence of low ($n_F < 1$), moderate ($1 < n_F < 2$) and high ($2 < n_F < 10$) adsorption capacities [45]. From the isothermal parameters displayed in Table 6, it can be seen, that both models were well fitted to experimental data ($R^2 > 0.90$). However, the Langmuir model was that best described the biosorption equilibrium data of red-120 presenting the highest value of determination coefficient (R^2 = 0.9461) and the lowest value of normalized standard deviation (Δq_e = 12.4%) which denotes that the biosorption capacity calculated by the model is close to the experimental. This model describes that monolayer biosorption maximum capacity (Q_m) of FB

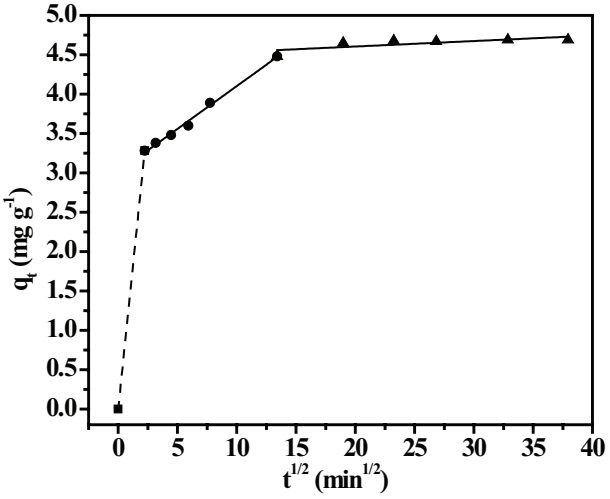

Fig. 8. Linear adjustments of intraparticle diffusion model for biosorption of red-120 onto FB.

Table 5
Kinetic parameters obtained from linear fit of the intraparticle diffusion model

C_0 (mg L^{-1})	First stage			Second stage			Third stage		
	k_{d1}	C_1	R^2	k_{d2}	C_2	R^2	k_{d3}	C_3	R^2
50	1.47	0	1	0.110	3.01	0.9925	0.010	4.47	0.4847

C_1, C_2 and C_3 are the intercepts associated with the boundary layer thickness (mg g^{-1}).

for red-120 was 44.44 mg g^{-1}. The advantage supporting the use of FB from the wild *Ganoderma* stipitatum as a feasible and environmentally friendly biosorbent is the elimination of reagents consumption.

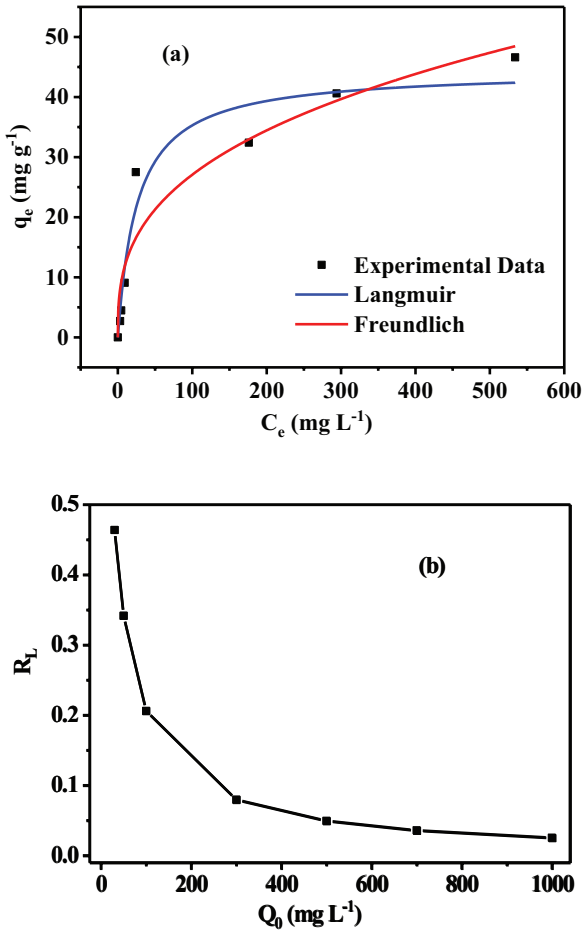

Fig. 9. Biosorption isotherm of red-120 onto FB and non-linear adjustments of Langmuir and Freundlich models (a) and Langmuir separation factor (R_L) (b).

Table 6
Isothermal parameters for the biosorption of red-120 onto FB

Model	Parameters	Values
Langmuir	$Q_{e,exp}$ (mg g^{-1})	46.6
	Q_m (mg g^{-1})	44.4
	K_L (L mg^{-1})	0.0385
	R^2	0.9461
	Δq_e (%)	12.4
Freundlich	K_F (L mg^{-1})	5.46
	n_F	2.88
	R^2	0.9095
	Δq_e (%)	16.5

The Langmuir separation factor, R_L, (Fig. 9(b)) is often used to classify the adsorption process as unfavorable ($R_L > 1$), linear ($R_L = 1$), favorable ($0 < R_L < 1$) or irreversible ($R_L = 0$) [55]. The values obtained for R_L were between 0 and 1 suggesting the favorability of red-120 biosorption in the concentration range studied (30–1,000 mg L^{-1}).

Table 7 shows values of maximum biosorption capacities (Q_m) of several biosorbents applied for removal of red-120 dye from aqueous solutions. As can be observed, the Q_m value of FB was of 44.44 mg g^{-1}, which is comparable with other materials reported in the literature.

3.2.4. Biosorption thermodynamics

The thermodynamic parameters provide important information regarding the biosorption process [60]. In case of negative values of $\Delta G°$, the biosorption is considered favorable and spontaneous; on the other hand, positive values of $\Delta G°$ indicate a non-spontaneous biosorption. Similarly, positive values of $\Delta H°$ suggest an endothermic process while negative values indicate the occurrence of an exothermic process. In addition, values of $\Delta S°$ denote the affinity between adsorbate and biosorbent, and spontaneity of process [61]. The thermodynamic parameters regarding the biosorption of red-120 onto FB are listed in Table 8. The $\Delta H°$ and $\Delta S°$ values were calculated from the slope $\left(\frac{-\Delta H°}{R}\right)$ and intercept $\left(\frac{\Delta S°}{R}\right)$, of the van't Hoff plot ($\ln K_c$ vs. $1/T$), respectively, which is shown in Fig. 10.

The negative values of $\Delta G°$ suggest the biosorption process occurred spontaneously and is favorably, while the negative value of $\Delta H°$ indicates its exothermic nature. The negative value of $\Delta S°$ is an indicative that there was no remarkable change in entropy, and that there was a decreased disorder at the solid–liquid interface of system red-120 and FB. The results herein found are agreeing with other works reported in the literature [62,63].

Table 7
Maximum biosorption capacities (Q_m) of biosorbents for removal of the red-120 from the aqueous solution

Biosorbent	Q_m (mg g^{-1})	Reference
Lentinus sajor-caju	117.8	[56]
Chara contraria	102.9	[57]
Spirogyra majuscula	41.20	[58]
Jatropha curcas shells	13.39	[59]
Ganoderma stipitatum	44.44	This work

Table 8
Thermodynamic parameters for red-120 biosorption onto FB

Temperature (K)	Parameters		
	$\Delta G°$ (kJ mol^{-1})	$\Delta H°$ (kJ mol^{-1})	$\Delta S°$ (kJ $mol^{-1} K^{-1}$)
298	–17.1	–75.2	–0.20
308	–14.3		
318	–10.9		
328	–10.9		
338	–9.02		

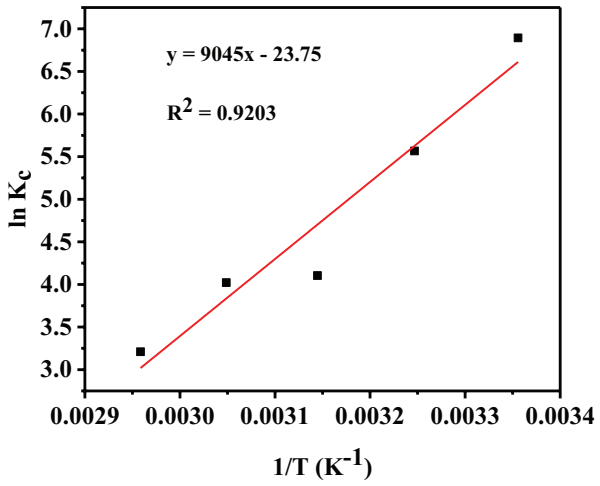

Fig. 10. van't Hoff plot for biosorption of red-120 onto FB.

4. Conclusion

The FB of *Ganoderma* stipitatum was applied as biosorbent for removal of reactive red-120 dye. The FB presented non-uniform filaments characteristics with specific surface area of 22.2 m^2 g^{-1} and chemical groups of triterpenes and polysaccharides. The surface charge characteristic of FB (pH_{PZC} = 6.5) favored the biosorption of red-120 in acidic pH. The kinetic studies demonstrated that the Elovich model was best fitted to experimental data, and that intraparticle diffusion could be involved along with other factors in the biosorption kinetics of red-120 onto FB, but it is not the rate-limiting step. The Langmuir model best described the equilibrium data, suggesting biosorption in monolayer with maximum biosorption capacity of 44.44 mg g^{-1}. In addition, the thermodynamic study evidenced the exothermic nature of biosorption process which was spontaneous and energetically favorable. Therefore, the results support the use of FB as biosorbent for removal of red-120 dye from wastewaters.

Acknowledgments

The authors acknowledge the financial support provided by the CAPES, Fundação Araucária-Paraná and CNPq-Brazil.

References

[1] T. Ngulube, J.R. Gumbo, V. Masindi, A. Maity, An update on synthetic dyes adsorption onto clay based minerals: a state-of-art review, J. Environ. Manage., 191 (2017) 35–57.
[2] V.K. Gupta, R. Kumar, A. Nayak, T.A. Saleh, M.A. Barakat, Adsorptive removal of dyes from aqueous solution onto carbon nanotubes: a review, Adv. Colloid Interface Sci., 193–194 (2013) 24–34.
[3] J. Paul, A.A. Kadam, S.P. Govindwar, P. Kumar, L. Varshney, An insight into the influence of low dose irradiation pretreatment on the microbial decolouration and degradation of Reactive Red-120 dye, Chemosphere, 90 (2013) 1348–1358.
[4] F.M. Amaral, M.T. Kato, L. Florêncio, S. Gavazza, Color, organic matter and sulfate removal from textile effluents by anaerobic and aerobic processes, Bioresour. Technol., 163 (2014) 364–369.
[5] A. Aouni, C. Fersi, B. Cuartas-Uribe, A. Bes-Pía, M.I. Alcaina-Miranda, M. Dhahbi, Reactive dyes rejection and textile effluent treatment study using ultrafiltration and nanofiltration processes, Desalination, 297 (2012) 87–96.
[6] R.T. Sapkal, S.S. Shinde, M.A. Mahadik, V.S. Mohite, T.R. Waghmode, S.P. Govindwar, K.Y. Rajpure, C.H. Bhosale, Photoelectrocatalytic decolorization and degradation of textile effluent using ZnO thin films, J. Photochem. Photobiol. B, 114 (2012) 102–107.
[7] A.N. Módenes, F.R. Espinoza-Quiñones, F.H. Borba, D.R. Manenti, Performance evaluation of integrated photo-Fenton – electrocoagulation process applied to pollutant removal from tannery effluent in batch system, Chem. Eng. J., 197 (2012) 1–9.
[8] H.M. Farzana, S. Meenakshi, Exploitation of zinc oxide impregnated chitosan beads for the photocatalytic decolorization of an azo dye, Int. J. Biol. Macromol., 72 (2015) 900–910.
[9] M.S. Mahmoud, M.K. Mostafa, S.A. Mohamed, N.A. Sobhy, M. Nasr, Bioremediation of red azo dye from aqueous solutions by *Aspergillus niger* strain isolated from textile wastewater, J. Environ. Chem. Eng., 5 (2017) 547–554.
[10] A.P. Singh, T. Singh, Biotechnological applications of wood-rotting fungi: a review, Biomass Bioenergy, 62 (2014) 198–206.
[11] A. Srinivasan, T. Viraraghavan, Decolorization of dye wastewaters by biosorbents: a review, J. Environ. Manage., 91 (2010) 1915–1929.
[12] Y. Fu, T. Viraraghavan, Fungal decolorization of dye wastewaters: a review, Bioresour. Technol., 79 (2001) 251–262.
[13] N.B. Colauto, F.A. Cordeiro, K.V.N. Geromini, T.G. Lima, A.D. Lopes, R.A.R. Nunes, F.B. Roratto, H.S. Tanaka, L.L. Zaghi Junior, G.A. Linde, Viability of *Agaricus blazei* after long-term cryopreservation, Ann. Microbiol., 62 (2012) 871–876.
[14] S. Brunauer, P.H. Emmet, E. Teller, Adsorption of gases in multimolecular layers, J. Am. Chem. Soc., 60 (1938) 309–319.
[15] P. Schneider, Adsorption isotherms of microporous-mesoporous solids revisited, Appl. Catal., A, 129 (1995) 157–165.
[16] E.P. Barrett, L.G. Joyner, P.P. Halenda, The determination of pore volume and area distributions in porous substances. I. Computations from nitrogen isotherms, J. Am. Chem. Soc., 73 (1951) 380–373.
[17] D. Prahas, Y. Kartika, N. Indraswati, S. Ismadji, Activated carbon from jackfruit peel waste by H_3PO_4 chemical activation: pore structure and surface chemistry characterization, Chem. Eng. J., 140 (2008) 32–42.
[18] S. Lagergren, About the theory of so-called adsorption of soluble substances, K. Sven. Vetensk.akad. Handl., 24 (1898) 1–39.
[19] G. Blanchard, M. Maunaye, G. Martin, Removal of heavy metals from waters by means of natural zeolites, Water Res., 18 (1984) 1501–1507.
[20] M.J.D. Low, Kinetics of chemisorption of gases on solids, Chem. Rev., 60 (1960) 267–312.
[21] W.J. Weber, J.C. Morris, Kinetics of adsorption on carbon from solution, J. Sanit. Eng. Div., 89 (1963) 31–60.
[22] I. Langmuir, The constitution and fundamental properties of solids and liquids. Part i. Solids, J. Am. Chem. Soc., 38 (1916) 2221–2295.
[23] H.M.F. Freundlich, Über die adsorption in lösungen, J. Chem. Phys., 57 (1906) 385–471.
[24] G. Crini, P.-M. Badot, Application of chitosan, a natural amino polysaccharide, for dye removal from aqueous solutions by adsorption processes using batch studies: a review of recent literature, Prog. Polym. Sci., 33 (2008) 399–447,
[25] Z. Aksu, Ş.Ş. Çağatay, Investigation of biosorption of Gemazol Turquise Blue-G reactive dye by dried *Rhizopus arrhizus* in batch and continuous systems, Sep. Purif. Technol., 48 (2006) 24–35.
[26] O. Hamdaoui, E. Naffrechoux, Modeling of adsorption isotherms of phenol and chlorophenols onto granular activated carbon Part II. Models with more than two parameters, J. Hazard. Mater., 147 (2007) 401–411.
[27] E. Smidt, K. Meissl, The applicability of Fourier transform infrared (FT-IR) spectroscopy in waste management, Waste Manage., 27 (2007) 268–276.
[28] D.A. Skoog, F.J. Holler, S.R. Crouch, Principles of Instrumental Analysis, 6th ed., Bookman, Porto Alegre, 2009, 1056 pp.
[29] N.B. Colthup, Spectra-structure correlations in the infra-red region, J. Opt. Soc. Am., 40 (1950) 397–400.

[30] Z. Movasaghi, S. Rehman, I. Urrehman, Fourier transform infrared (FTIR) spectroscopy of biological tissues, Appl. Spectrosc. Rev., 43 (2008) 134–179.
[31] E. Pehlivan, T. Altun, S. Cetin, M.I. Bhanger, Lead sorption by waste biomass of hazelnut and almond shell, J. Hazard. Mater., 167 (2009) 1203–1208.
[32] H. Schulz, M. Baranska, Identification and quantification of valuable plant substances by IR and Raman spectroscopy, Vib. Spectrosc., 43 (2007) 13–25.
[33] Y.K. Choong, S.-Q. Sun, Q. Zhou, Z. Ismail, B.A.A. Rashid, J.-X. Tao, Determination of storage stability of the crude extracts of *Ganoderma lucidum* using FTIR and 2D-IR spectroscopy, Vib. Spectrosc., 57 (2011) 87–96.
[34] M. Thommes, K. Kaneko, A.V. Neimark, J.P. Olivier, F. Rodriguez-Reinoso, J. Rouquerol, K.S.W. Sing, Physisorption of gases, with special reference to the evaluation of surface area and pore size distribution (IUPAC Technical Report), Pure Appl. Chem., 87 (2015) 1051–1069.
[35] M. Wawrzkiewicz, P. Bartczak, T. Jesionowski, Enhanced removal of hazardous dye form aqueous solutions and real textile wastewater using bifunctional chitin/lignin biosorbent, Int. J. Biol. Macromol., 99 (2017) 757–764.
[36] C. Ribeiro, F.B. Scheufele, F.R. Espinoza-Quinones, A.N. Módenes, M.G.C. Silva, M.G.A. Vieira, C.E. Borba, Characterization of *Oreochromis niloticus* fish scales and assessment of their potential on the adsorption of reactive blue 5G dye, Colloids Surf., A, 482 (2015) 693–701.
[37] C.M.M.S. Silva, I.S. Mel, P.R. Oliveira, Ligninolytic enzyme production by *Ganoderma* spp., Enzyme Microb. Technol., 37 (2005) 324–329.
[38] D. Palin Jr., K.B. Rufato, G.A. Linde, N.B. Colauto, J. Caetano, O. Alberton, D.A. Jesus, D.C. Dragunski, Evaluation of Pb (II) biosorption utilizing sugarcane bagasse colonized by *Basidiomycetes*, Environ. Monit. Assess., 5 (2016) 188–279.
[39] O. Pezoti, A.L. Cazetta, K.C. Bedin, L.S. Souza, A.C. Martins, T.L. Silva, O.O.S. Junior, J.V. Visentainer, V.C. Almeida, NaOH-activated carbon of high surface area produced from guava seeds as a high-efficiency adsorbent for amoxicillin removal: kinetic, isotherm and thermodynamic studies, Chem. Eng. J., 288 (2016) 778–788.
[40] Lj.S. Čerović, S.K. Milonjić, M.B. Todorović, M.I. Trtanj, Y.S. Pogozhev, Y. Blagoveschhenskii, E.A. Levashov, Point of zero charge of different carbides, Colloids Surf., A, 297 (2007) 1–6.
[41] A. Çelekli, B. Tanriverdi, H. Bozkurt, Predictive modeling of removal of Lanaset Red G on *Chara contraria*; kinetic, equilibrium, and thermodynamic studies, Chem. Eng. J., 169 (2011) 166–172.
[42] K.M.G. Machado, L.C.A. Compart, R.O. Morais, L.H. Rosa, M.H. Santos, Biodegradation of reactive textile dyes by basidiomycetous fungi from Brazilian ecosystems, Braz. J. Microbiol., 37 (2006) 481–487.
[43] R.D. Koyani, G.V. Sanghvi, R.K. Sharma, K.S. Rajput, Contribution of lignin degrading enzymes in decolourisation and degradation of reactive textile dyes, Int. Biodeterior. Biodegrad., 77 (2013) 1–9.
[44] S.S. Gupta, K.G. Bhattacharyya, Kinetics of adsorption of metal ions on inorganic materials: a review, Adv. Colloid Interface Sci., 162 (2011) 39–58.
[45] O. Pezoti, A.L. Cazetta, K.C. Bedin, L.S. Souza, R.P. Souza, S.R. Melo, V.C. Almeida, Percolation as new method of preparation of modified biosorbents for pollutants removal, Chem. Eng. J., 283 (2016) 1305–1314.
[46] T.A. Khan, S.A. Chaudhry, I. Ali, Equilibrium uptake, isotherm and kinetic studies of Cd(II) adsorption onto iron oxide activated red mud from aqueous solution, J. Mol. Liq., 202 (2015) 165–175.
[47] A.M.M. Vargas, A.L. Cazetta, A.C. Martins, J.C.G. Moraes, E.E. Garcia, G.F. Gauze, W.F.C. Costa, V.C. Almeida, Kinetic and equilibrium studies: adsorption of food dyes Acid Yellow 6, Acid Yellow 23, and Acid Red 18 on activated carbon from flamboyant pods, Chem. Eng. J., 181–182 (2012) 243–250.
[48] S. Nethaji, A. Sivasamy, Adsorptive removal of an acid dye by lignocellulosic waste biomass activated carbon: equilibrium and kinetic studies, Chemosphere, 82 (2011) 1367–1372.
[49] B.-E. Wang, Y.-Y. Hu, L. Xie, K. Peng, Biosorption behavior of azo dye by inactive CMC immobilized *Aspergillus fumigatus* beads, Bioresour. Technol., 99 (2008) 794–800.
[50] X. Xiao, F. Zhang, Z. Feng, S. Deng, Y. Wang, Adsorptive removal and kinetics of Methylene Blue from aqueous solution using NiO/MCM-41 composite, Phys. E, 65 (2015) 4–12.
[51] G. Bayramoğlu, G. Çelik, M.Y. Arica, Biosorption of Reactive Blue 4 dye by native and treated fungus *Phanerochaete chrysosporium*: batch and continuous flow system studies, J. Hazard. Mater., 137 (2006) 1689–1697.
[52] N. Caner, I. Kiran, S. Ilhan, C.F. Iscen, Isotherm and kinetic studies of Burazol Blue ED dye biosorption by dried anaerobic sludge, J. Hazard. Mater., 165 (2009) 279–284.
[53] K.V. Kumar, V. Ramamurthi, S. Sivanesan, Modeling the mechanism involved during the sorption of Methylene Blue onto fly ash, J. Colloid Interface Sci., 284 (2005) 14–21.
[54] C. Mckay, A. Mesdaghinia, S. Nasseri, M. Hadi, M.S. Aminabad, Optimum isotherms of dyes sorption by activated carbon: fractional theoretical capacity & error analysis, Chem. Eng. J., 251 (2014) 236–247.
[55] O. Pezoti Jr., A.L. Cazetta, I.P.A.F. Souza, K.C. Bedin, A.C. Martins, T.L. Silva, V.C. Almeida, Adsorption studies of Methylene Blue onto $ZnCl_2$-activated carbon produced from Buriti shells (*Mauritia flexuosa* L.), J. Ind. Eng. Chem., 20 (2014) 4401–4407.
[56] M.Y. Arica, G. Bayramoğlu, Biosorption of Reactive Red-120 dye from aqueous solution by native and modified fungus biomass preparations of *Lentinus sajor-caju*, J. Hazard. Mater., 149 (2007) 499–507.
[57] A. Çelekli, G. Ilgüna, H. Bozkurt, Sorption equilibrium, kinetic, thermodynamic, and desorption studies of Reactive Red 120 on *Chara contraria*, Chem. Eng. J., 191 (2012) 228–235.
[58] A. Çelekli, M. Yavuzatmaca, H. Bozkurt, Kinetic and equilibrium studies on biosorption of Reactive Red 120 from aqueous solution on *Spirogyra majuscula*, Chem. Eng. J., 152 (2009) 139–145.
[59] L.D.T. Prola, E. Acayank, E.C. Lima, C.S. Umpierres, J.C.P. Vaghetti, W.O. Santos, S. Laminsi, P.T. Djifon, Comparison of *Jatropha curcas* shells in natural form and treated by non-thermal plasma as biosorbents for removal of Reactive Red 120 textile dye from aqueous solution, Ind. Crops Prod., 46 (2013) 328–340.
[60] A. Özcan, E.M. Öncü, A.S. Özcan, Kinetics, isotherm and thermodynamic studies of adsorption of Acid Blue 193 from aqueous solutions onto natural sepiolite, Colloids Surf., A, 277 (2006) 90–97.
[61] V.K. Gupta, A. Mittal, V. Gajbe, Adsorption and desorption studies of a water soluble dye, Quinoline Yellow, using waste materials, J. Colloid Interface Sci., 284 (2005) 89–98.
[62] D. Mitrogiannis, G. Markou, A. Celekli, H. Bozkurt, Biosorption of methylene blue onto *Arthrospira platensis* biomass: kinetic, equilibrium and thermodynamic studies, J. Environ. Chem. Eng., 3 (2015) 670–680.
[63] T.L. Silva, A.L. Cazetta, P.S.C. Souza, T. Zhang, T. Asefa, V.C. Almeida, Mesoporous activated carbon fibers synthesized from denim fabric waste: efficient adsorbents for removal of textile dye from aqueous solutions, J. Cleaner Prod., 171 (2018) 482–490.